Journal of Nuclear Medicine, published on November 19, 2015 as doi:10.2967/jnumed.115.164442

[68Ga]PSMA-HBED PET for differential diagnosis of suspicious lung lesions in patients with prostate cancer

Thomas Pyka[1,*,†], Gregor Weirich[2,†] Ingo Einspieler[1], Tobias Maurer[3], Jörg Theisen[4], Georgios Hatzichristodoulou[3], Kristina Schwamborn[2], Markus Schwaiger[1] and Matthias Eiber[1]

[1]Department of Nuclear medicine, Klinikum rechts der Isar der TU München, Ismaninger Str., Munich, Germany

[2]Institute of Pathology, Klinikum rechts der Isar der TU München, Ismaninger Str., Munich, Germany

[3]Department of Urology, Klinikum rechts der Isar der TU München, Ismaninger Str., Munich, Germany

[4]Department of Surgery, Klinikum rechts der Isar der TU München, Ismaninger Str., Munich, Germany

*corresponding author:
Thomas Pyka MD MSc
Department of Nuclear medicine
Klinikum rechts der Isar der TU München
Ismaninger Str. 22
81675 Munich
Germany
mail: thomas.pyka@tum.de
telephone: +49 89 4140 2972
fax: +49 89 4140 4950

†equally contributing

Wordcount

total: 3596, abstract: 263

PSMA PET for lung lesions in PC

Abstract

Rationale

In prostate cancer (PC) patients, differentiation between lung metastases and lesions of different origin, e.g. primary lung cancer, is a common clinical question. Herein we investigate the use of ^{68}Ga-PSMA-HBED-CC for this purpose.

Methods

1889 PC patients receiving ^{68}Ga-PSMA PET/CT or PET/MR scans were evaluated retrospectively for suspicious lung lesions. For up to 5 lesions per patient, location, CT diameter, CT morphology and SUVmax values were determined. Standard for classification was either histopathologic evaluation or, in case of PC metastases, responsivity to anti-hormone therapy. Comparison of the different classes was executed by Student's t test. PSA and PSMA immunohistochemistry were performed if histologic samples were available; ^{68}Ga -PSMA autoradiography was performed on an exemplary case of PET positive lung cancer.

Results

89 lesions in 45 patients were identified, of which 76 were classified as PC (39 proven, 37 highly probable), 7 as primary lung cancer and 2 as activated tuberculosis; 4 lesions remained unclear. The mean SUVmax was 4.4±3.9 for PC metastases and 5.6±1.6 for primary lung cancer ($p=0.408$). Additionally, substantial differences in SUVmax values intra-individually were detected. The two tuberculous lesions showed an SUVmax of 7.8 and 2.5, respectively. Using immunohistochemistry, we could demonstrate PSMA expression in the neo-vasculature of

several PSMA PET positive lung cancers, as well as in tuberculous lesions from our histologic database.

Conclusion

Quantitative (SUV) analysis of ^{68}Ga-PSMA PET was not able to discriminate reliably between pulmonary metastases and primary lung cancer in PC patients. The reason for the unexpectedly high tracer uptake in non-PC lesions is not completely clear. PSMA expression in neo-vasculature provides a possible explanation for this finding; however, other contributing factors, such as tracer binding to proteins other than PSMA, cannot be excluded at present.

Keywords

68Ga-PSMA; prostate cancer; pulmonary metastasis; lung cancer

Introduction

Radio-labelled prostate-specific membrane antigen (PSMA) ligands are increasingly used in the work-up of patients with prostate cancer (PC). PSMA, or glutamate carboxypeptidase II, is a membrane bound protein expressed in the prostate and a variety of other tissues (*1, 2*). It shows significantly elevated expression levels in PC compared to benign prostatic cells (*3*), making it a promising target for molecular imaging. Glu-NH-CO-NH-Lys(Ahx)-HBED-CC (^{68}Ga-PSMA-HBED-CC) is an extracellular PSMA inhibitor combining an urea-based binding motif with an interaction between the HBED-CC chelator and a lipophilic pocket in the extracellular PSMA domain (*4*). PET with ^{68}Ga-labelled PSMA-HBED-CC has been shown to be of high clinical value for lymph node staging and detection of local recurrence in PC patients, resulting in detection rates of up to 97 % depending on PSA levels (*5, 6*). Although these excellent results are consistent with a high specificity based on preclinical studies (*7*), there have also been reports on tracer enhancement in benign lesions and other tumor entities (*8, 9*). This phenomenon has been attributed mainly to PSMA expression in neo-vasculature and specialized (e.g. endocrine) cells as demonstrated by immunohistochemistry (*3*).

Visceral metastases are encountered less often than lymph node or bone metastases and occur predominantly in the later course of disease (*10*), but affect prognosis severely (*11*) and may lead to changes in the therapeutic regimen. The predominant sites of visceral metastases in a post-mortem study were lung (46 % of patients with distant metastases), liver (25 %), pleura (21 %) and adrenals (13 %) (*12*). Differentiation between PC metastases and lesions of different origin using conventional imaging may be challenging and, in many cases, warrants histologic clarification. Imaging options for lung nodules are especially restricted, as only plain x-ray, CT

and FDG PET are clinically established for this purpose (*13*) – the last, though, is of limited value in PC (*14*). Herein we investigate the value of ^{68}Ga-PSMA PET for the diagnostic work-up of suspicious lung nodules in PC patients and evaluate whether the high specificity of PSMA PET can help in identifying pulmonary PC metastases.

Material and Methods

Patients

From a total number of 1889 individuals who underwent ^{68}Ga-PSMA-ligand PET/CT or PET/MR for staging or restaging of PC from the institutions´ database (11/2012 to 03/2015), patients with suspicious pulmonary nodules in CT were extracted retrospectively. Only intrapulmonary lesions, but no thoracic lymph nodes were analyzed. Lesions with a maximum diameter of < 7 mm were excluded to minimize partial volume effects in PET (*15*); in addition, lesions had to be either increasing in size compared to earlier CT scans, multiple lesions, or irregularly configured. Stable nodules compared to previous or follow-up CT without specific therapy as well as those with classical signs of benignity (fat or calcification) were excluded.

All patients gave written informed consent for the purpose of anonymized evaluation and publication of their data. The retrospective analysis was approved by the institutional review board of the Technical University of Munich (permit 5665/13).

Classification

Lesions were classified into the groups ‘PC all’, which was further divided into ‘PC highly probable’ and ‘PC proven’, ‘lung cancer’, ‘other entity’ and ‘unclear’ (see Tables 1 and 2).

Diagnosis of PC metastases was 'proven' either by histology or if pulmonary lesions showed clear regression under anti-hormone therapy. If these criteria were not fulfilled, 'PC metastases highly probable' was chosen for multiple suspicious lung lesions in a patient with other distant metastases, no other known malignancy and elevated PSA levels. 'Lung cancer' was reserved for lesions with a conclusive histology. The class 'other entity' was chosen for lesions with a conclusive histology or sputum analysis proving a non-PC origin. The remaining suspicious lung lesions were classified as 'unclear'.

Synthesis and application of ^{68}Ga-PSMA ligand

Images were obtained with HBED-CC (*7*) that was labelled with $^{68}Ga^{3+}$ (half-life 67.6 min) from a ^{68}Ge/^{68}Ga radionuclide generator (iThemba Labs, South Africa) by means of a fully automated module (Scintomics, Germany) and good manufacturing practice grade disposable cassettes and reagent kit (ABX, Germany) as described previously (*16*). The final product was dissolved in isotonic phosphate-buffered saline (PBS) with subsequent sterile filtration.

The ^{68}Ga-PSMA-ligand complex solution was applied to patients via an intravenous bolus (mean 151±30 MBq, range 95–236 MBq). Variation of injected radiotracer activity was caused by the short half-life of ^{68}Ga and variable elution efficiencies obtained during the lifetime of the ^{68}Ge/^{68}Ga radionuclide generator.

Imaging protocol

PET acquisition was started at a mean time of 54.7 ± 8.5 min after tracer injection (median 54 min; range 45 – 80 minutes). 41 patients underwent ^{68}Ga -PSMA PET/CT on a Biograph mCT scanner (Siemens Medical Solutions, Erlangen, Germany) and 4 patients ^{68}Ga PSMA PET/MR on

a Biograph mMR scanner (Siemens Medical Solutions, Erlangen, Germany. PET/CT and PET/MR acquisitions were performed as previously described (*5, 17*). Notably, for evaluation of lung lesions an inspiratory CT of the thorax was acquired in PET/CT and an axial contrast-enhanced T1w VIBE-sequence in PET/MR; additional inspiratory CT acquisitions were available for all PET/MR patients. All PET-images were acquired in 3D mode and reconstructed by an attenuation-weighted ordered-subsets expectation maximization algorithm (four iterations, eight subsets) followed by a post-reconstruction smoothing Gaussian filter (5 mm full-width at half-maximum).

Image analysis

For up to five suspicious lung lesions per patient, starting from the biggest, location, morphology, CT diameter and SUVmax in PSMA PET were obtained. ^{68}Ga -PSMA-ligand PET and CT or MR images were read by one board certified nuclear medicine physician and one board certified radiologist, followed by a final consensus read.

Statistical analysis

For the different classes of lesions as described above, SUVmax values were analyzed and box-and-whisker plots were created. SUVmax values of the classes 'PC all' and 'PC proven' were compared to the class 'lung cancer' using Student's t test. Tests were performed two-sided and a level of significance of α=0.05 was used. Statistical analyses were conducted with GraphPad Prism 6.1 (GraphPad Software Inc., La Jolla, CA).

Histology

For histologic evaluation, all specimens from our imaged cohort, as well as two exemplary cases

of tuberculosis from our histologic database were fixed in 10% buffered formalin and paraffin embedded according to standard procedures. 3µm tissue sections were subsequently stained with H&E and PAS (periodic acid-Schiff stain) for diagnostic purposes. Immunohistochemistry used anti-PSMA antibodies (clone 3E6, Dako, Carpinteria, CA; clone 7E11, kindly provided by Dr. Grimm, Memorial Sloan Kettering Cancer Center, NY) and PSA-antiboides (polyclonal rabbit anti-human PSA antibody, Dako, Carpinteria, CA**)** to label prostate cancer cells. An automated immunostaining device (BenchMark XT IHC/ISH, Ventana, Germany) was used according to the manufacturer's protocol (XT ultraView DAB v3) employing a citrate buffer (pH 6.0) and DAB (diaminobenzidine) as chromogen, as well as haemtatoxylin for counterstaining.

For autoradiography, the fresh frozen tissue of one exemplary case of primary lung cancer which had shown a clear signal in PSMA PET was cryosectioned in 15 µm slices, fixed in Delauney's solution for 1 min and air dried. Afterwards, the specimens were incubated with 30 kBq/ml ^{68}Ga-PSMA-HBED-CC in HEPES buffer (25 mM, pH 7.4). Exposure was for 4 h on a BAS-IP TR 2025 E Tritium screen (Fujifilm, Stamford, CT).

Results

45 patients who exhibited suspicious lung lesions were identified. According to the criteria defined above, in 18 patients lesions were classified as 'PC proven', in 15 as 'PC highly probable' and in 8 as 'other entity' (7 cases of lung cancer and 1 case of reactivated tuberculosis). In 3 patients, the origin of the lung lesions remained unclear. Please see 'classification' in the methods for details on how the classes were defined. There were no cases in which multiple classifications in one patient were present. Patient details are listed in Table 1.

The total number of suspicious pulmonary lesions was 89. Detailed lesions characteristics are given in Table 2. 39 lesions were classified as 'PC proven' 37 lesions as 'PC highly probable', 7 as 'lung cancer proven' and 2 as 'other entity' (both resembling activated tuberculous lesions according to sputum analysis). 4 lesions remained 'unclear'. The mean SUVmax was 4.3±3.7 for all lesions, 4.4±3.9 for all PC metastases, 5.0±4.4 for histologically proven PC metastases and 5.6±1.6 for proven primary lung carcinoma. The two tuberculous lesions showed an SUVmax of 7.8 and 2.5, respectively.

Figures 1 and 2 show imaging examples of patients with pulmonary PC metastasis (PSMA PET/CT) and primary lung cancer (PSMA and FDG PET/CT). Interestingly, the latter also exhibited two mediastinal lymph nodes which were positive in both PSMA and FDG PET scans, and which represented histologically proven lymph node metastases. Please note this represents only an illustrative case for which lymph node uptake was evaluated, and it was not included into the statistical analysis.

No significant difference in SUVmax comparing lung cancer with all PC ($p=0.408$; see Fig. 3) or lung cancer with histologically proven PC only ($p=0.740$) was observed, although an SUVmax of ≥ 8 (9 out of 89 lesions) occurred only in prostate cancer metastases. An intra-individual comparison in patients with multiple lesions showed large differences in SUV between different nodules in one patient (see Fig. 4), which cannot be attributed solely to partial volume effects – e. g. patient 1 exhibited an SUVmax from 3.1 to 20.4 while all lesions were 12 to 13 mm in diameter. Morphology was not distinctive either, as, although all primary lung cancers had an irregular or spiculated appearance, this morphologic feature was also demonstrated in 27 (35.6 %) of 76 PC metastases.

PSMA immunohistochemistry was evaluated for the primary non-small cell lung cancers in our cohort. We could detect PSMA expression in tumor-associated neo-vasculature in all specimens (Fig. 6d). PSA immunohistochemistry was also performed, but was negative for all samples. Furthermore, we extracted two cases of tuberculosis from our histologic database and could also demonstrate PSMA positive vessels (Fig. 7). No other cell-specific PSMA antibody binding was detected.

Postoperative PSMA autoradiography was established on frozen slices of PC tissue (Fig. 5, unpublished data). This procedure was used for an exemplary PSMA PET positive lung tumor from the imaged cohort (SUVmax 5.2) for which fresh frozen tissue was available. The PSA blood level was 0.44 ng/ml; histologic evaluation classified this tumor as a primary adenocarcinoma of the lung. Diffuse PSMA tracer binding was detected in autoradiography which was apparently not limited to blood vessels (Fig. 6).

Discussion

In this study, we retrospectively investigated the potential value of ^{68}Ga-PSMA-HBED-CC PET/CT for the differential diagnosis of suspicious lung lesions in PC patients. The differentiation of potentially malignant pulmonary lesions is of considerable clinical importance; the occurrence of distant metastases adversely affects the prognosis of PC patients and will often lead to modifications in the treatment regime, mostly systemic anti-hormone or chemotherapy. On the other hand, primary lung carcinoma, the second most common malignant tumor in males, is potentially curable by resection. Conventional imaging options for thoracic lesions are restricted, with only plain x-ray and CT being used in common clinical practice. The reported

high specificity of PSMA PET for lymph node staging in PC patients raises expectations of a similar usefulness for the diagnosis of pulmonary metastases.

Our results do not support these expectations. Conversely, we found an unanticipated high PSMA PET uptake in primary lung tumors. Although in our cohort only PC metastases showed an SUVmax of > 8, a clear differentiation between PC metastases and primary lung cancer, e. g. by an SUVmax cut-off is not possible according to our data. The specificity of PSMA PET is further challenged by pronounced tracer uptake in two lesions resembling activated tuberculosis. Sensitivity was not as high as expected either, as a number of proven pulmonary PC metastases showed only faint uptake in PSMA PET, which might be explained in part by response to previous therapies. However, as a consequence, all suspicious lesions, whether exhibiting uptake in PSMA PET or not, should either be followed up by CT or PET/CT or clarified by biopsy.

We should underline here that it was not the purpose of this study to differentiate between benign and malignant lesions by PSMA PET. Considering the inclusion criteria, it is evident that many common benign lesions, such as post-inflammatory scars or granulomas, were excluded from the study. In fact, besides the two tuberculous lesions, there were no cases of proven benign nodules in our cohort, though some of the 'unclear' lesions may well have been non-malignant.

The reason for PSMA HBED-CC tracer enhancement in non-PC lesions is not completely clear: free ^{68}Ga binding e. g. to CD71 was considered, but seems rather unlikely due to the high radiochemical purity of the injected tracer. Using immunohistochemistry we could demonstrate PSMA expression in the neo-vasculature of PSMA PET positive lung carcinomas, a phenomenon that has been reported before for different tumors (*18*). Furthermore, and rather unexpectedly,

we could also show PSMA immunostaining in the neo-vasculature of two exemplary cases of tuberculosis from our histologic database; reports on PSMA expression in non-neoplastic regenerative tissue can as well be found in the literature (*19*). The low density of PSMA positive vessels, however, casts some doubt on the hypothesis that this phenomenon alone is responsible for the considerable amount of PSMA tracer uptake seen in these lesions. The doubts are substantiated by the demonstration of diffuse tracer binding in an exemplary autoradiography of a primary lung tumor from our cohort, while PSMA expression in lung tumor cells, though reported previously (*20*), could not be verified. This result raises the question whether binding to a substance other than PSMA might be a possible contributing factor. Natural candidate proteins would include PSMA homologs, such as glutamate carboxypeptidase III (*21, 22*) or N-acetylated α-linked acidic dipeptidase-like protein (NAALADase L) (*23*). Further insight could be gained by performing tracer uptake assays on tumor cell lines, therefore excluding the effect of tracer binding to neo-vasculature.

Our study is limited by its retrospective nature and the relatively low number of proven non-PC lesions in the investigated cohort. In addition, we cannot exclude that, in some cases, biopsies of unclear lesions were sought due to high uptake in PET imaging, which might have induced further bias. However, we think that the most important implication – the lack of discriminative power of PSMA HBED-CC PET-imaging regarding the underlying histology of suspicious lung lesions – is not critically affected by these limitations.

Conclusion

Quantitative analysis of ^{68}Ga-PSMA-HBED-PET was not able to discriminate reliably between pulmonary lesions of different origin in PC patients. Primary lung tumors showed unexpectedly high tracer uptake similar to PC metastases. PSMA expression in neo-vasculature provides a possible explanation for these findings; however, other contributing factors, such as tracer binding to proteins other than PSMA, cannot be excluded at present.

Disclosure

This study was supported by funding from the Faculty of Medicine of the Technical University of Munich (grant to TP: KKF B11-14). MS has received funding from the European Union Seventh Framework Program (FP7) under Grant Agreement No. 294582 ERC Grant MUMI. The development of ^{68}Ga-PSMA synthesis was supported by SFB 824 (Project Z1) from the Deutsche Forschungsgemeinschaft, Bonn, Germany. The research leading to these results has received funding from the European Union Seventh Framework Program (FP7) under Grant Agreement No. 256984 EndoTOFPET.

References

1. Mhawech-Fauceglia P, Zhang S, Terracciano L, et al. Prostate-specific membrane antigen (PSMA) protein expression in normal and neoplastic tissues and its sensitivity and specificity in prostate adenocarcinoma: an immunohistochemical study using mutiple tumour tissue microarray technique. *Histopathology.* 2007;50:472-483.

2. Wright GL, Jr., Haley C, Beckett ML, Schellhammer PF. Expression of prostate-specific membrane antigen in normal, benign, and malignant prostate tissues. *Urol Oncol.* 1995;1:18-28.

3. Silver DA, Pellicer I, Fair WR, Heston WD, Cordon-Cardo C. Prostate-specific membrane antigen expression in normal and malignant human tissues. *Clin Cancer Res.* 1997;3:81-85.

4. Kularatne SA, Zhou Z, Yang J, Post CB, Low PS. Design, synthesis, and preclinical evaluation of prostate-specific membrane antigen targeted (99m)Tc-radioimaging agents. *Mol Pharm.* 2009;6:790-800.

5. Eiber M, Maurer T, Souvatzoglou M, et al. Evaluation of hybrid 68Ga-PSMA-ligand PET/CT in 248 patients with biochemical recurrence after radical prostatectomy. *J Nucl Med.* 2015.

6. Afshar-Oromieh A, Avtzi E, Giesel FL, et al. The diagnostic value of PET/CT imaging with the (68)Ga-labelled PSMA ligand HBED-CC in the diagnosis of recurrent prostate cancer. *Eur J Nucl Med Mol Imaging.* 2015;42:197-209.

7. Eder M, Schafer M, Bauder-Wust U, et al. 68Ga-complex lipophilicity and the targeting property of a urea-based PSMA inhibitor for PET imaging. *Bioconjug Chem.* 2012;23:688-697.

8. Schwenck J, Tabatabai G, Skardelly M, et al. In vivo visualization of prostate-specific membrane antigen in glioblastoma. *Eur J Nucl Med Mol Imaging.* 2015;42:170-171.

9. Krohn T, Verburg FA, Pufe T, et al. [(68)Ga]PSMA-HBED uptake mimicking lymph node metastasis in coeliac ganglia: an important pitfall in clinical practice. *Eur J Nucl Med Mol Imaging.* 2015;42:210-214.

10. Moschini M, Sharma V, Zattoni F, et al. Natural History of Clinical Recurrence Patterns of Lymph Node-Positive Prostate Cancer After Radical Prostatectomy. *Eur Urol.* 2015.

11. Goodman OB, Jr., Flaig TW, Molina A, et al. Exploratory analysis of the visceral disease subgroup in a phase III study of abiraterone acetate in metastatic castration-resistant prostate cancer. *Prostate Cancer Prostatic Dis.* 2014;17:34-39.

12. Bubendorf L, Schopfer A, Wagner U, et al. Metastatic patterns of prostate cancer: an autopsy study of 1,589 patients. *Hum Pathol.* 2000;31:578-583.

13. Gould MK, Donington J, Lynch WR, et al. Evaluation of individuals with pulmonary nodules: when is it lung cancer? Diagnosis and management of lung cancer, 3rd ed: American College of Chest Physicians evidence-based clinical practice guidelines. *Chest.* 2013;143:e93S-120S.

14. Jadvar H. Imaging evaluation of prostate cancer with 18F-fluorodeoxyglucose PET/CT: utility and limitations. *Eur J Nucl Med Mol Imaging.* 2013;40 Suppl 1:S5-10.

15. Kessler RM, Ellis JR, Jr., Eden M. Analysis of emission tomographic scan data: limitations imposed by resolution and background. *J Comput Assist Tomogr.* 1984;8:514-522.

16. Schafer M, Bauder-Wust U, Leotta K, et al. A dimerized urea-based inhibitor of the prostate-specific membrane antigen for 68Ga-PET imaging of prostate cancer. *EJNMMI Res.* 2012;2:23.

17. Souvatzoglou M, Eiber M, Martinez-Moeller A, et al. PET/MR in prostate cancer: technical aspects and potential diagnostic value. *Eur J Nucl Med Mol Imaging.* 2013;40 Suppl 1:S79-88.

18. Chang SS, Reuter VE, Heston WD, Bander NH, Grauer LS, Gaudin PB. Five different anti-prostate-specific membrane antigen (PSMA) antibodies confirm PSMA expression in tumor-associated neovasculature. *Cancer Res.* 1999;59:3192-3198.

19. Gordon IO, Tretiakova MS, Noffsinger AE, Hart J, Reuter VE, Al-Ahmadie HA. Prostate-specific membrane antigen expression in regeneration and repair. *Mod Pathol.* 2008;21:1421-1427.

20. Wang HL, Wang SS, Song WH, et al. Expression of prostate-specific membrane antigen in lung cancer cells and tumor neovasculature endothelial cells and its clinical significance. *PLoS One.* 2015;10:e0125924.

21. Hlouchova K, Barinka C, Klusak V, et al. Biochemical characterization of human glutamate carboxypeptidase III. *J Neurochem.* 2007;101:682-696.

22. Tykvart J, Schimer J, Jancarik A, et al. Design of highly potent urea-based, exosite-binding inhibitors selective for glutamate carboxypeptidase II. *J Med Chem.* 2015;58:4357-4363.

23. Tykvart J, Barinka C, Svoboda M, et al. Structural and biochemical characterization of a novel aminopeptidase from human intestine. *J Biol Chem.* 2015;290:11321-11336.

Figures

Figure 1 – Example PSMA PET/CT scan of a patient with pulmonary PC metastasis

A– CT shows an irregularly shaped lesion in the left upper lobe in a PC patient after radical prostatectomy, no known metastases and PSA of 1,58 ng/ml. The lesions was subsequently biopsied and diagnosed as pulmonary PC metastasis; B– PSMA PET is positive with an SUVmax of 7.1; C– PET/CT fusion image

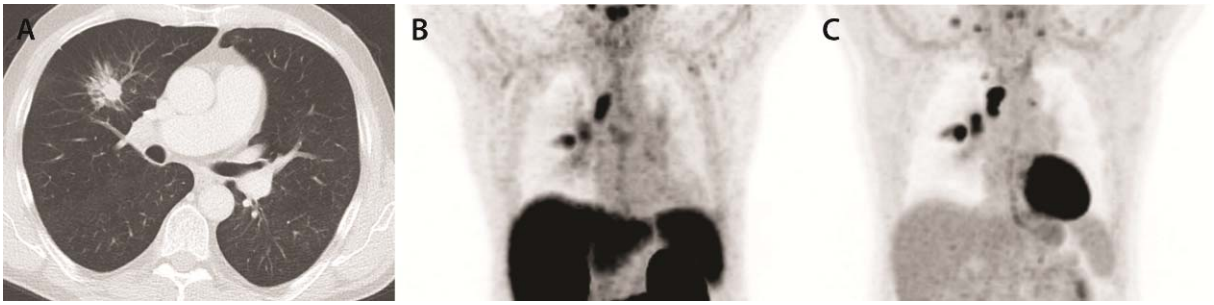

Figure 2 – Example PET/CT scans of a patient with primary lung cancer (adenocarcinoma)

A – CT shows a spiculated lesion in the right upper lobe in a PC patient after prostatectomy and suspected local recurrence; PSA was 4,09 ng/ml; B – PSMA-PET exhibits focal tracer enhancement in the pulmonary lesion (SUVmax 5.3) and in two mediastinal lymph nodes, which were histologically confirmed as primary lung cancer and associated lymph node metastases. Please note this was the only case for which lymph node uptake was evaluated; C – FDG-PET as the established imaging method of choice for lung cancer shows similar enhancement in the primary tumor and the two mediastinal lymph node metastases.

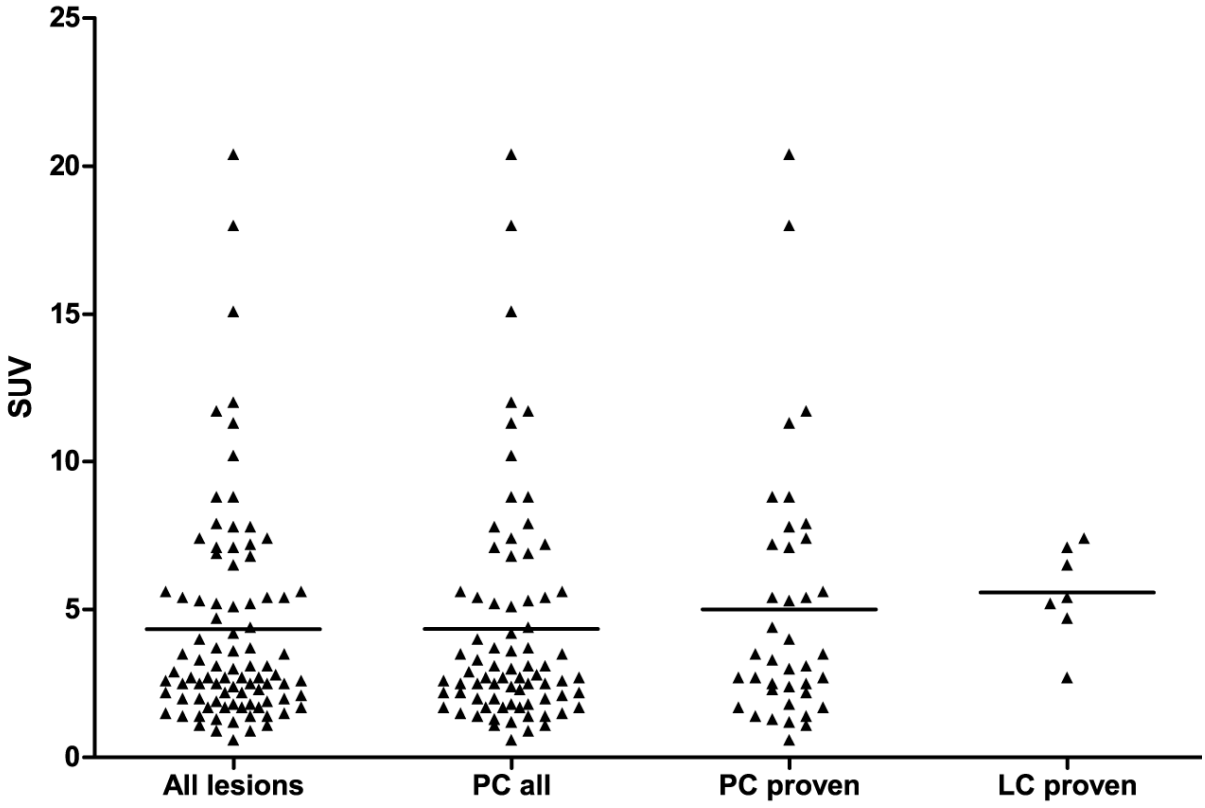

Figure 3 - Distribution of SUVmax values for different lesion classes

No significant difference was shown when comparing SUVmax distributions between groups 'PC all' (n=76) consisting of 'PC proven' and 'PC highly probable' vs. 'lung cancer proven' (n=7) (p=0.408) and 'PC proven' (n=39) only vs. 'lung cancer proven' (p=0.780)

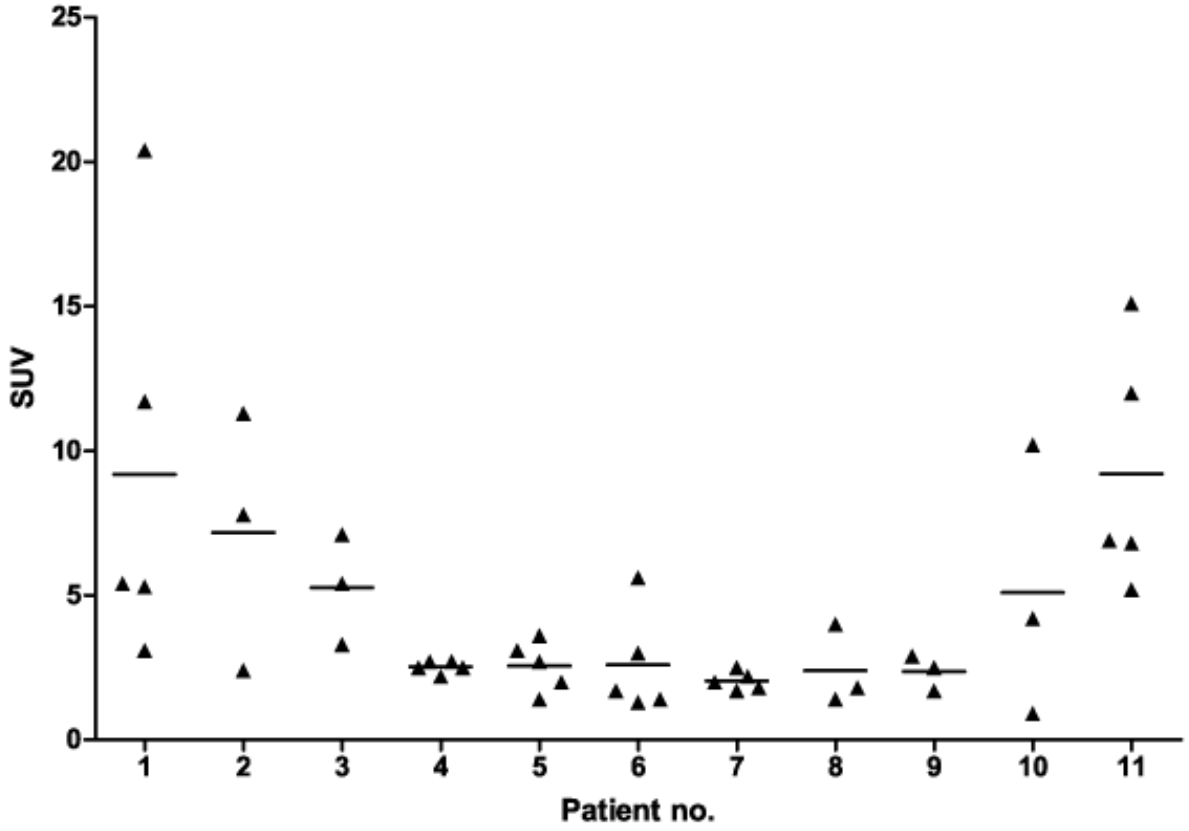

Figure 4 – Intraindividual variability of PSMA uptake in pulmonary PC metastases

Shown is the distribution of SUVmax values for proven or probable pulmonary PC metastases in patients exhibiting 3 or more lesions

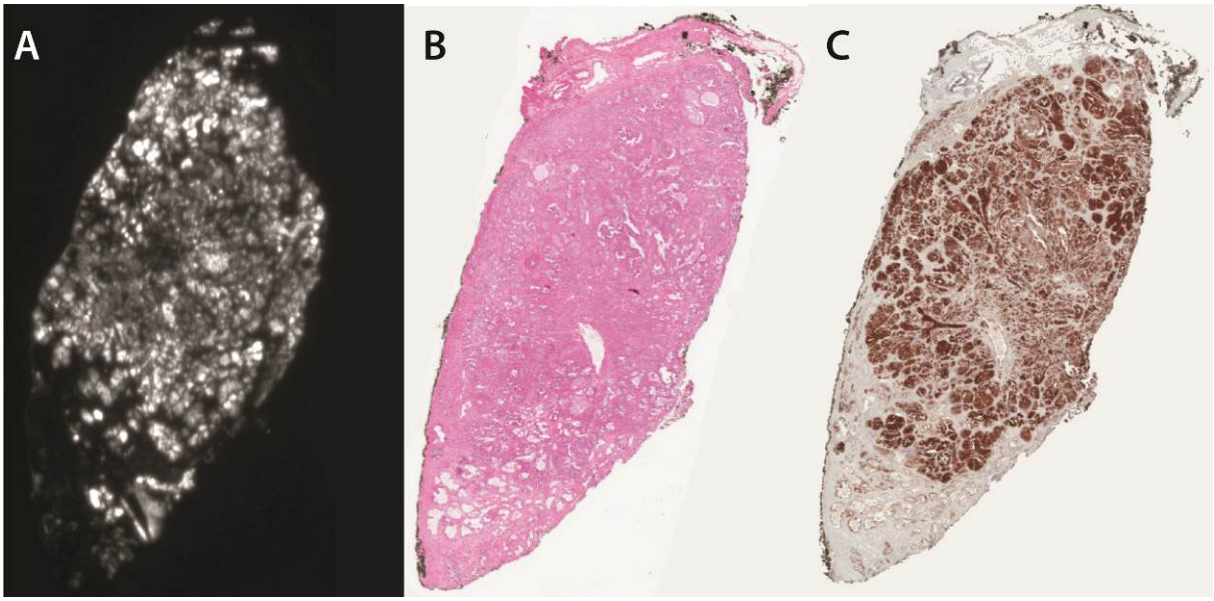

Figure 5 – ^{68}Ga-PSMA autoradiography and PSMA immunohistochemistry of a prostate carcinoma

PC samples were used to establish autoradiography and immunohistology protocols A – PSMA autoradiography. B – HE stain, C – Immunohistochemistry with anti-PSMA antibody 7E11 (aliquot kindly provided by Dr. Grimm, Memorial Sloan Kettering Cancer Center, NY)

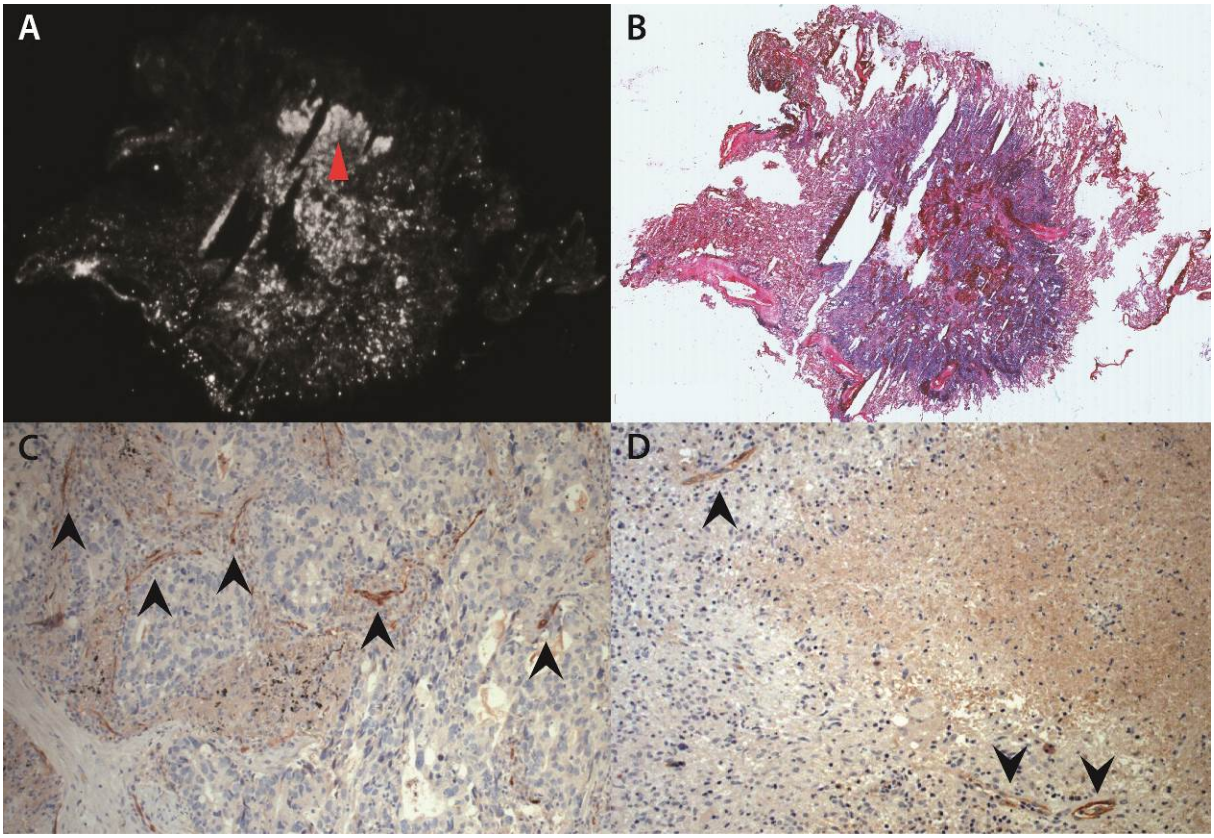

Figure 6 - Autoradiography and PSMA immunohistochemistry of an exemplary case of primary lung cancer and PSMA immunohistology of a tuberculous lesion

A – PSMA autoradiography of a primary lung carcinoma from the imaged cohort which exhibited a strong signal in PSMA PET (SUVmax 5.2), B – HE stain showing the tumor contours, C – PSMA immunohistochemistry of the same tumor, showing a detail of a tumor region with high cell density and high signal in autoradiography (red arrowhead in A), exhibiting no tumor cells with clear PSMA expression, but PSMA in neo-vasculature (black arrowheads) D – PSMA immunohistochemistry of a case of active tuberculosis from our histologic database, showing PSMA positive blood vessels (black arrowheads)

Tables

Table 1 - Patients

Number	N = 45
Age [years]	68.8 (50 – 83)
PSA [ng/ml]	5.67 (0.2 – 18000)
Injected Dose [MBq]	151 (97 – 236)
Classification	
PC proven	**18**
by histology	7
by therapy response	11
other entity proven	**8**
NSCLC	7
Tbc	1
PC highly probable	**15**
unclear	**4**

Table 2 - Lesion characteristics

	all	PC all	PC proven	LC proven	other/unclear
Number of lesions	89	76	39	7	6
Localisation					
Rt. UL	22	16	10	5	1
Rt. LL	19	17	9	1	1
ML	4	4	1	0	0
Lt. UL	25	22	14	1	2
Lt. LL	19	17	5	0	2
Configuration					
smooth	41	39	14	0	2
lobulated	11	10	5	0	1
irregular	30	26	19	1	3
speculated	7	1	1	6	0
CT diam. [mm]	12.5±6.3	11.8±5.6	13.2±6.9	21.0±9.2	11.7±1.8
SUV_{max}	4.3±3.7	4.4±3.9	5.0±4.4	5.5±1.9	2.7±2.5

UL – upper lobe, ML – middle lobe, LL – lower lobe